Journal of Engineering Physics and Thermophysics, Vol. 76, No. 2, 2003

PROBLEM OF MASS TRANSFER IN THE CASE OF SUPERDEEP PENETRATION

S. K. Andilevko

UDC 534.2

The loss in the mass of a particle in the process of its motion in the material of an obstacle is estimated on the basis of the superdeep-penetration model.

As has been noted in [1], further theoretical investigation of the superdeep-penetration phenomenon is hindered by the absence of any information on the process of change in the mass of particles moving in the material of an obstacle. At the same time, the data of the experimental investigations [2, 3] incontestably point to the fact that the size and mass of the particles decrease as a result of their penetration. This is because of the friction accompanying the interaction of the particles with the flow of the softened material of the obstacle [1].

It has been established [1] that in the case of fulfillment of the necessary and sufficient conditions of superdeep penetration, when the velocity of a particle falls within the range

$$U_{\min} \le U \le U_{\max}\,, \tag{1}$$

where

$$U_{\max} = \sqrt{\frac{p}{\rho}}\,, \quad U_{\min} = \frac{ad}{\Delta^2}\,, \tag{2}$$

the particle (object) moves in the obstacle material uniformly without meeting resistance. If the velocity of the object is $U > U_{\max}$, it is rapidly retarded in the obstacle until U is equal to $U_{\max}$, whereupon the object moves uniformly unless it collides with inclusions contained in the actual material of the obstacle [1]. If the velocity of the particle is lower than $U_{\min}$, it is incapable of making the obstacle material in its vicinity softer and will stop very rapidly without traversing a distance larger than 5–10d. When the velocity of the particle is higher than $U_{\max}$, the stage of its retarded motion is very short and lasts for $\sim 2\text{–}4\cdot 10^{-8}$ sec [1, 2], whereupon the stage of uniform motion begins and lasts, according to [1], much longer — as long as several hundred microseconds. Thus, it is obvious that the largest change in the mass of the particle occurs at the stage of uniform motion, which makes the problem much simpler. Since the entire friction energy of the softened-material flux incident on the particle is expended in heating the particle and changing its mass, the law of conservation of energy of the particle–obstacle system can be written as

$$\frac{d}{dt}\,(MU^2) + \varepsilon_{\rm s}\,\frac{dM}{dt} = c_{\rm f}\,\rho\,\frac{U^3}{2}\,S\,. \tag{3}$$

The mechanism of loss in the mass of a striker can qualitatively be described in the following way. In the process of penetration, the material of the particle is heated in the zones adjacent to the contact surface between the two materials due to friction. With time, the heating changes to melting, the liquid film is carried by the slip flow to the back critical point where it separates from the surface of the particle. This is integrally described by the equation

$$\frac{U^2}{2}\,dM + c_p\,(T_{\rm m} - T_0)\,dM + q_{\rm m}dM + \varepsilon_{\rm m}\,dM = c_{\rm f}\,\rho\,\frac{U^3}{2}\,S\,, \tag{4}$$

A. V. Luikov Heat and Mass Transfer Institute, National Academy of Sciences of Belarus, Minsk, Belarus. Translated from Inzhenerno-Fizicheskii Zhurnal, Vol. 76, No. 2, pp. 19–23, March–April, 2003. Original article submitted October 21, 2002.

1062-0125/03/7602-0251$25.00

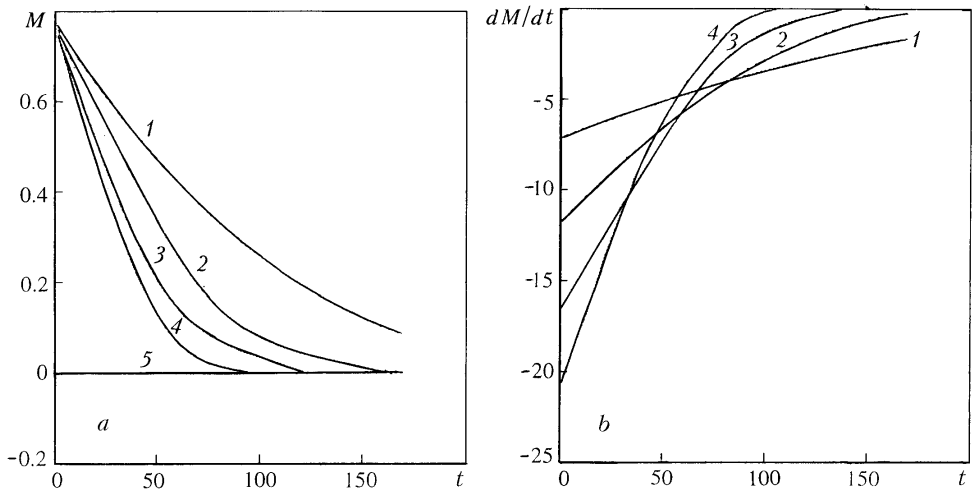

Fig. 1. Change in the particle mass (a) and rate of this change (b) versus time for: 1) U = 300, 2) 500, 3) 700, and 4) 900 m/sec; 5) corresponds to the zero level. M, μg; dM/dt, mg/sec; t, μsec.

whence it follows that

$$\frac{dM}{S} = \frac{c_f U dt}{1 + 2\dfrac{c_p (T_m - T_0) + q_m + \varepsilon_m}{U^2}} \frac{\rho}{\rho_p}. \tag{5}$$

For a spherical particle we have

$$dM = 4\pi R^2 dR, \quad S = \pi R^2. \tag{6}$$

Substituting (6) into (5), we obtain the differential equation

$$dR = \frac{0.25 c_f U dt}{1 + 2\dfrac{c_p (T_m - T_0) + q_m + \varepsilon_m}{U^2}} \frac{\rho}{\rho_p}, \tag{7}$$

whose integration gives

$$R(t) = R_0 \left[\frac{0.25 c_f}{1 + 2\dfrac{c_p (T_m - T_0) + q_m + \varepsilon_m}{U^2}} \frac{\rho}{\rho_p} \frac{Ut}{R_0} \right] \tag{8}$$

and

$$M(t) = \frac{4}{3}\pi R(t)^3 \quad \text{and} \quad dM = 4\pi R(t)^2 dR. \tag{9}$$

Figure 1 shows the $M(t)$ and dM/dt curves for different values of the velocity U (it is assumed that $\varepsilon_m \ll q_m$). As is seen, the higher the velocity, the higher the rate of loss in the mass of the particles.

In the calculations that follow, we will use the results of [1], which demonstrate that the general character of the process can be described using the curves of the velocities U_{min}, U_p, and U_{max}. In this work (see Fig. 2), we present the velocity curves for steel, aluminum, and lead specimens loaded by a particle flux formed by a conical accelerator. The dependence of the number of particles in the flux loading the surface of the obstacle on the interaction

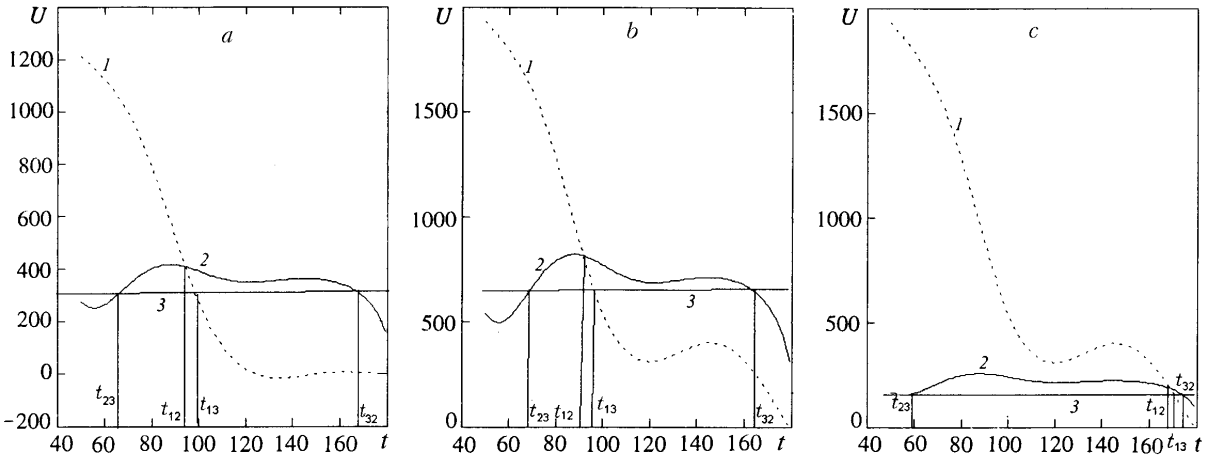

Fig. 2. Curves of the velocity of particle motion for specimens of steel (a), aluminum (b), and lead (c) which are treated with a bronze-particle flux generated by an accelerator of powder with a conical recess: 1) U_p; 2) U_{max}; 3) U_{min}. U, m/sec; t, μsec.

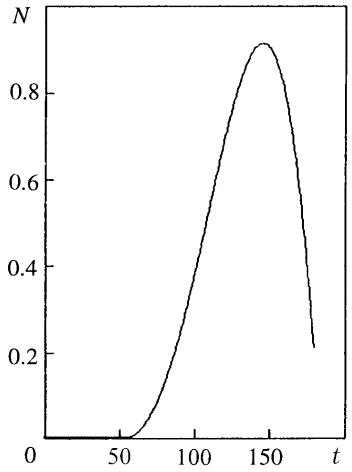

Fig. 3. Dependence of the number of the flux particles coming to the unit area of the obstacle per unit time on the interaction time. N, 10^9 ($mm^{-2} \cdot sec^{-1}$); t, μsec.

time $N(t)$ is presented in Fig. 3. Denoting the time intervals of interaction of the flux with the obstacle by t_{12}, t_{13}, t_{23}, and t_{32} (instants of time corresponding to the intersection of curves 1 and 2 and 1 and 3, the first intersection of curves 2 and 3, and the second intersection of curves 3 and 2), as is shown in Fig. 2, we determine the quantitative characteristics of the penetrating flux by the method developed in [1]. The number of highest-velocity particles that do not penetrate into the obstacle by the superdeep-penetration mechanism because of the low background pressure is calculated as

$$N_{out} = \int_{t_0}^{t_{23}} N(\Theta)\, d\Theta \tag{10}$$

and accounts for 169, 93, and 155 particles per mm^2 for steel, lead, and aluminum respectively. The numbers of particles penetrating into the obstacle by the superdeep-penetration mechanism

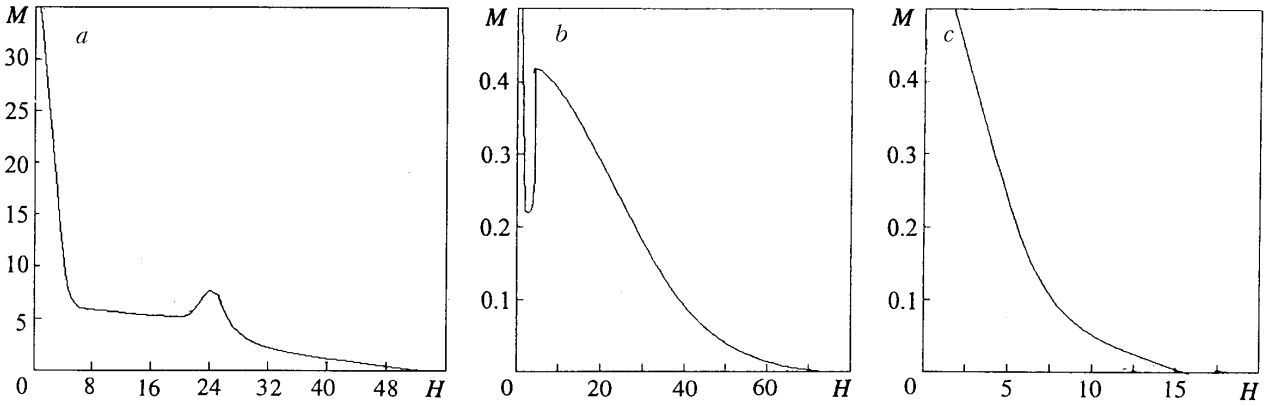

Fig. 4. Distribution of the introduced-material mass over the depth for steel (a), aluminum (b), and lead (c). M, μg/mm^2; H, mm.

$$N_{\text{SDP}} = \int_{t_{23}}^{t_{12}} N(\Theta)\, d\Theta + \int_{t_{12}}^{t_{13}} N(\Theta)\, d\Theta , \tag{11}$$

will be 467 and 225 particles per mm^2 for steel and aluminum respectively, which is in good agreement with the data of [2]. Now we can pass to the calculation of such parameters as the distribution of the mass and the number of penetrating flux particles over the depth of the obstacle. Let us determine the time layers δt in the time interval t_{23}–t_{13}, where

$$\delta t = \frac{d}{U} . \tag{12}$$

Let each layer from t to $t + \delta t$ correspond to the number of particles

$$n(t) = \int_{t}^{t+\delta t} N(\Theta)\, d\Theta , \tag{13}$$

their mass

$$m(t) = M(t)\, n(t) \tag{14}$$

and the mass lost in this layer by the particles that were able to pass through it and move further:

$$\Delta m(t) = \int_{t_{23}}^{t} N(\Theta)\, \Delta M(\Theta)\, d\Theta , \tag{15}$$

where

$$\Delta M = M(t) - M(t + \delta t) . \tag{16}$$

We now find the depth of penetration of the particles of each layer:

$$H(t) = \int_{t_{32}-t}^{t_{32}} U_{\text{SDP}}(\Theta)\, d\Theta , \tag{17}$$

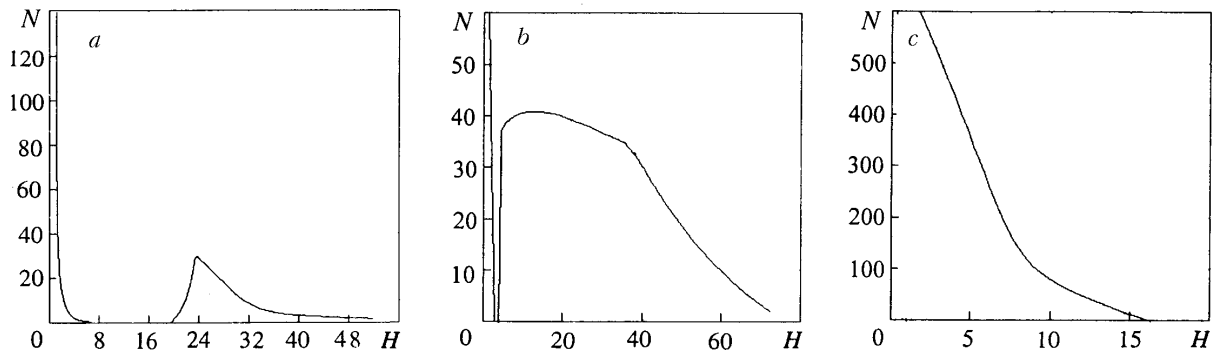

Fig. 5. Distribution of the particles introduced into the obstacle over the depth for steel (a), aluminum (b), and lead (c). N, mm^{-2}; H, mm.

where

$$U_{\mathrm{SDP}}(\Theta) = \begin{cases} U_{\max}(\Theta), & U \geq U_{\max}; \\ U(t), & U_{\min} \leq U < U_{\max}. \end{cases} \tag{18}$$

Having calculated numerically all the above-indicated parameters, we can calculate the dependences of the number of penetrating particles and the introduced mass on the depth of the obstacle. The total mass introduced into the layer considered will be determined as

$$m_{\mathrm{SDP}}(t) = m(t) + \Delta m(t). \tag{19}$$

Figure 4 shows the change in the mass introduced into the obstacle material versus the penetration depth for obstacles of steel, aluminum, and lead. Figure 5 contains data on the distribution of the number of penetrating particles over the depth in the same order: for steel, aluminum, and lead. It is seen from Fig. 5a and b that in the process of penetration into these materials, a large number of particles (several tens of thousands) are jammed in the near-surface layers of the obstacle. But as they bite deeper into the obstacle, their number decreases very rapidly; for steel, $N(t)$ becomes negligibly small (practically equal to zero) at a depth of 6–7 mm. For aluminum, this depth is determined at 4–5 mm. Then the curve of the number of particles experiences a jump (at a depth of 24 mm for steel and at a depth of 8–9 mm for aluminum) and thereafter begins to smoothly and rapidly drop in both cases. This discontinuity in the penetration is due to the fact that the part of the flux corresponding to the time interval from t_{13} to t_{32} does not penetrate into the obstacle ($U < U_{\min}$), although in its parameters it is precisely this part of the flux that could fill the lacuna formed. At the same time, such a lacuna is not formed for lead (Figs. 4c and 5c). The dependence of the mass of the flux material introduced into the obstacle on the depth of the latter is made up of two dependences: the dependence of the mass of the particles jammed in this case and the dependence of the mass of the material lost by the particles which passed through this layer in transit on the obstacle depth. Therefore, as is seen from Fig. 4a and b, the mass of the introduced material decreases slightly on the portion from 6 to 24 mm for steel and on the portion from 5 to 8 mm for aluminum. Then, in both cases, the mass increases abruptly, and thereafter decreases smoothly but rapidly. For lead, the distribution of the mass of the introduced material, as well as the distribution of the penetrating particles, remains a smooth monotonically decreasing function.

The calculation data presented in Figs. 4 and 5 are in good agreement with the data of the direct experiments [2, 3] in the order of magnitude of the mass of the penetrating flux and of the inclusions revealed in the obstacle. Thus, the superdeep-penetration model based on the numerical model of gas-powder flow [2, 4, 5] can successfully be used as the first approximation for description of the process of superdeep penetration. To develop further the superdeep-penetration theory, it is necessary to have a more exact model of the flux generated by an explosive accelerator which would take into account the pattern of internal collisions in the flux, the order of its interaction with the obstacle, and the influence of the processes caused by the blocking of the obstacle and sticking of powder particles to its surface on this interaction. The availability of such information will make it possible to develop an exact and exhaus-

tive model of superdeep penetration and to fruitfully use it for development of new technological processes in the field of production of composite materials.

The author is grateful to V. A. Shilkin and G. S. Romanov for their active participation in the discussion and for all kinds of support of this work.

NOTATION

a, thermal diffusivity of the obstacle, m^2/sec; U and d, velocity and initial diameter of the particle, m/sec and m; p, pressure generated in the obstacle by a particle flux, GPa; ρ, density, kg/m^3; N, number of particles passing through a cross section of 1 mm^2 per unit time, 1/(mm^2·sec); S and M, midsection and mass of the particle, mm^{-2} and kg; Δ, width of the slip plane of the obstacle material, m; ε_s, energy necessary for heating, melting, and separation of a unit mass of the particle from its surface, J/kg; c_f, coefficient of friction on the contact surface particle–softened obstacle material; c_p and q_m, heat capacity and latent heat of melting of the particle material, J/(kg·K) and J/kg; T_m and T_0, melting and initial temperatures, K; ε_m, specific energy of separation of the melt from the surface of the particle, J/kg; t, running time, sec; R and R_0, running and initial radii of the particle, m; Θ, integration parameter; δt, thickness of the time layer, sec; $n(t)$, number of particles in a given time layer; $m(t)$, mass of all the particles settled in a given time layer, μg; $\Delta M(t)$, change in the mass of an individual particle in a given time layer (mass of the introduced material left by an individual particle in the layer), μg; $\Delta m(t)$, mass of the introduced material left in the layer by all the particles passed through it, μg. Subscripts: p, parameter of the particle; out, parameter characterizing a result that is not related to superdeep penetration; 0, initial value of the quantity; max, maximum; min, minimum; s, surface; m, melt; f, friction; SDP, superdeep penetration.

REFERENCES

1. S. K. Andilevko, *Inzh.-Fiz. Zh.*, **76**, No. 2, 12–18 (2003).
2. O. V. Roman, S. K. Andilevko, and S. S. Karpenko, *Scientific Report* No. 19992123, Minsk (1999).
3. O. V. Roman, S. K. Andilevko, and S. S. Karpenko, *Khim. Fiz.*, **21**, No. 9, 50–54 (2002).
4. O. V. Roman, O. A. Dybov, and S. K. Andilevko, *Inzh.-Fiz. Zh.*, **73**, No. 4, 797–801 (2000).
5. O. V. Roman, S. K. Andilevko, and S. S. Karpenko, *Inzh.-Fiz. Zh.*, **74**, No. 2, 73–79 (2001).